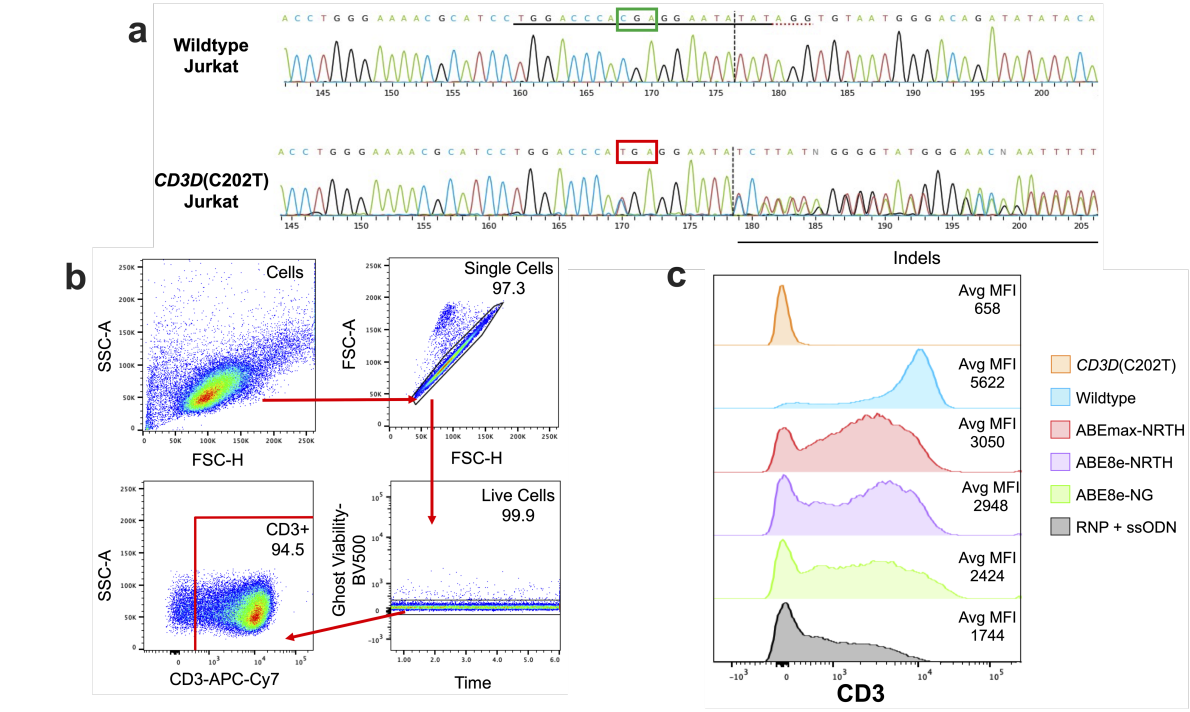

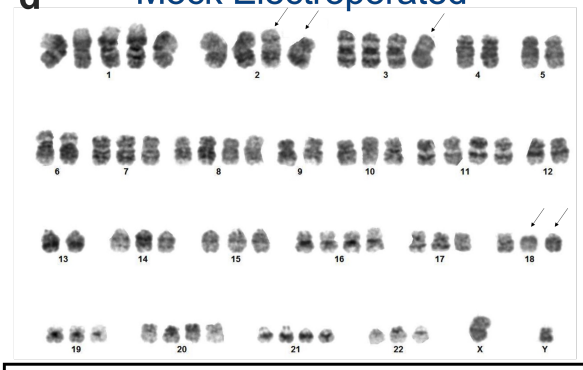

59~80<3n>,XXY,+1,+2,del(2)(p23p21)x2,+3,add(3(p25)x2,-5,-6,+6, +8,-9,+11,+12,-13,+13,+14,+16,add(18)(p11.2)x2,+20,+21,-22[cp5]

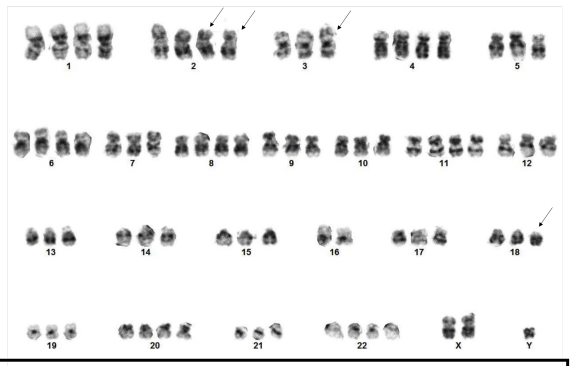

76~79<3n>,XXY,+1,+2,del(2)(p23p21)x2,+3,add(3)(p25), +4,+6,+7, +8,+11,+12,add(18)(p11.2),+20,+22[cp3]

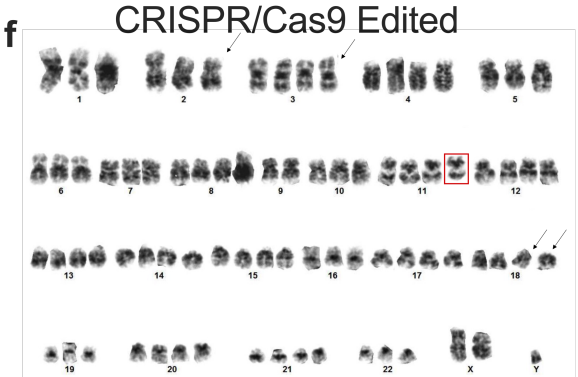

59~80<3n>,XXY,-Y,+1,+2,del(2)(p23p21)x2,+3,add(3)(p25),+4,-5,+6,+7,+8, -9,+10,+11,del(11)(q23), -12,+12,+13,+14,+15,+16,+17,+18,add(18)(p11.2)x2, -19,+20,+21,-22[cp7]

Figure S1. Base Editing Efficiently Restores CD3 Expression without Inducing Chromothripsis, Related to Fig. 1

a) Sanger sequencing traces confirm knockin of the *CD3D* c.202C>T pathogenic mutation in *CD3D* alleles with the remaining three alleles containing disruptive indels induced by CRISPR-mediated DSBs (rendering the latter three alleles uneditable, and therefore could be omitted from HTS analysis). Traces show the sense strand read 5' to 3'. The black dashed vertical line represents the Cas9 cut site during CRISPR editing, with approximately 150,000 total reads per population. **b)** Representative flow cytometry plots for CD3 surface expression. Top right: gating strategy to distinguish single cells. Bottom right: live cells. Bottom left: gating strategy to identify cells expressing CD3. SSC-A, side scatter area; FSC-A, forward scatter area; FSC-H, forward scatter height. **c)** Flow cytometry histogram profiling mean fluorescence intensity (MFI) of CD3 expression in CD3D(C202T) Jurkat T cells (orange), wildtype Jurkat T cells (blue), and ABEmax-NRTH (red), ABE8e-NRTH (purple), ABE8e-NG (green), and RNP + ssODN-treated cells (black). G-banded karyotypes each representing clonal abnormalities observed in cells from **d)** mock electroporated, **e)** base-edited with plasmids encoding ABEmax-NRTH and sgRNA, or **f)** edited with Cas9 RNP and ssODN. Due to the complexity of the cell lines, the clonal abnormalities are described as composite karyotypes (not all indicated abnormalities were identified in all abnormal cells analyzed) using standard cytogenetic nomenclature (ISCN). Diploid, triploid, and tetraploid cells were observed. Black arrows indicate clonal structural abnormalities inherent to the Jurkat T cell line.

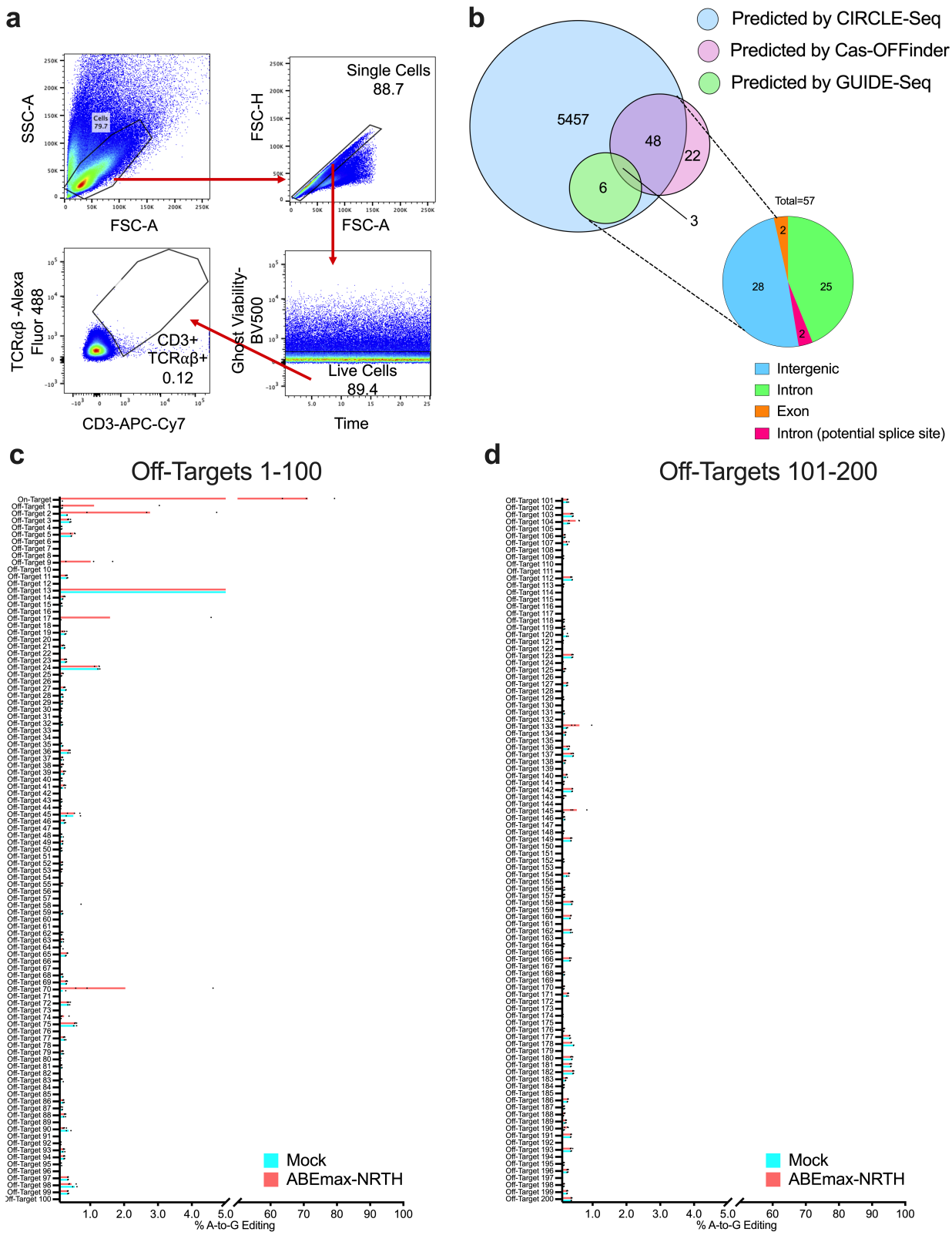
a
SSC-A
FSC-A
Cells
79.7
FSC-H
FSC-A
Single Cells
88.7
TCRαβ -Alexa Fluor 488
CD3-APC-Cy7
CD3+
TCRαβ+
0.12
Ghost Viability-BV500
Time
Live Cells
89.4
b
Predicted by CIRCLE-Seq
Predicted by Cas-OFFinder
Predicted by GUIDE-Seq
5457
48
22
6
3
Total=57
2
28
25
2
Intergenic
Intron
Exon
Intron (potential splice site)
c
Off-Targets 1-100
On-Target
Off-Target 1
Off-Target 2
Off-Target 3
Off-Target 4
Off-Target 5
Off-Target 6
Off-Target 7
Off-Target 8
Off-Target 9
Off-Target 10
Off-Target 11
Off-Target 12
Off-Target 13
Off-Target 14
Off-Target 15
Off-Target 16
Off-Target 17
Off-Target 18
Off-Target 19
Off-Target 20
Off-Target 21
Off-Target 22
Off-Target 23
Off-Target 24
Off-Target 25
Off-Target 26
Off-Target 27
Off-Target 28
Off-Target 29
Off-Target 30
Off-Target 31
Off-Target 32
Off-Target 33
Off-Target 34
Off-Target 35
Off-Target 36
Off-Target 37
Off-Target 38
Off-Target 39
Off-Target 40
Off-Target 41
Off-Target 42
Off-Target 43
Off-Target 44
Off-Target 45
Off-Target 46
Off-Target 47
Off-Target 48
Off-Target 49
Off-Target 50
Off-Target 51
Off-Target 52
Off-Target 53
Off-Target 54
Off-Target 55
Off-Target 56
Off-Target 57
Off-Target 58
Off-Target 59
Off-Target 60
Off-Target 61
Off-Target 62
Off-Target 63
Off-Target 64
Off-Target 65
Off-Target 66
Off-Target 67
Off-Target 68
Off-Target 69
Off-Target 70
Off-Target 71
Off-Target 72
Off-Target 73
Off-Target 74
Off-Target 75
Off-Target 76
Off-Target 77
Off-Target 78
Off-Target 79
Off-Target 80
Off-Target 81
Off-Target 82
Off-Target 83
Off-Target 84
Off-Target 85
Off-Target 86
Off-Target 87
Off-Target 88
Off-Target 89
Off-Target 90
Off-Target 91
Off-Target 92
Off-Target 93
Off-Target 94
Off-Target 95
Off-Target 96
Off-Target 97
Off-Target 98
Off-Target 99
Off-Target 100
Mock
ABEmax-NRTH
1.0
2.0
3.0
4.0
5.0
60
70
80
90
100
% A-to-G Editing
d
Off-Targets 101-200
Off-Target 101
Off-Target 102
Off-Target 103
Off-Target 104
Off-Target 105
Off-Target 106
Off-Target 107
Off-Target 108
Off-Target 109
Off-Target 110
Off-Target 111
Off-Target 112
Off-Target 113
Off-Target 114
Off-Target 115
Off-Target 116
Off-Target 117
Off-Target 118
Off-Target 119
Off-Target 120
Off-Target 121
Off-Target 122
Off-Target 123
Off-Target 124
Off-Target 125
Off-Target 126
Off-Target 127
Off-Target 128
Off-Target 129
Off-Target 130
Off-Target 131
Off-Target 132
Off-Target 133
Off-Target 134
Off-Target 135
Off-Target 136
Off-Target 137
Off-Target 138
Off-Target 139
Off-Target 140
Off-Target 141
Off-Target 142
Off-Target 143
Off-Target 144
Off-Target 145
Off-Target 146
Off-Target 147
Off-Target 148
Off-Target 149
Off-Target 150
Off-Target 151
Off-Target 152
Off-Target 153
Off-Target 154
Off-Target 155
Off-Target 156
Off-Target 157
Off-Target 158
Off-Target 159
Off-Target 160
Off-Target 161
Off-Target 162
Off-Target 163
Off-Target 164
Off-Target 165
Off-Target 166
Off-Target 167
Off-Target 168
Off-Target 169
Off-Target 170
Off-Target 171
Off-Target 172
Off-Target 173
Off-Target 174
Off-Target 175
Off-Target 176
Off-Target 177
Off-Target 178
Off-Target 179
Off-Target 180
Off-Target 181
Off-Target 182
Off-Target 183
Off-Target 184
Off-Target 185
Off-Target 186
Off-Target 187
Off-Target 188
Off-Target 189
Off-Target 190
Off-Target 191
Off-Target 192
Off-Target 193
Off-Target 194
Off-Target 195
Off-Target 196
Off-Target 197
Off-Target 198
Off-Target 199
Off-Target 200
Mock
ABEmax-NRTH
1.0
2.0
3.0
4.0
5.0
60
70
80
90
100
% A-to-G Editing

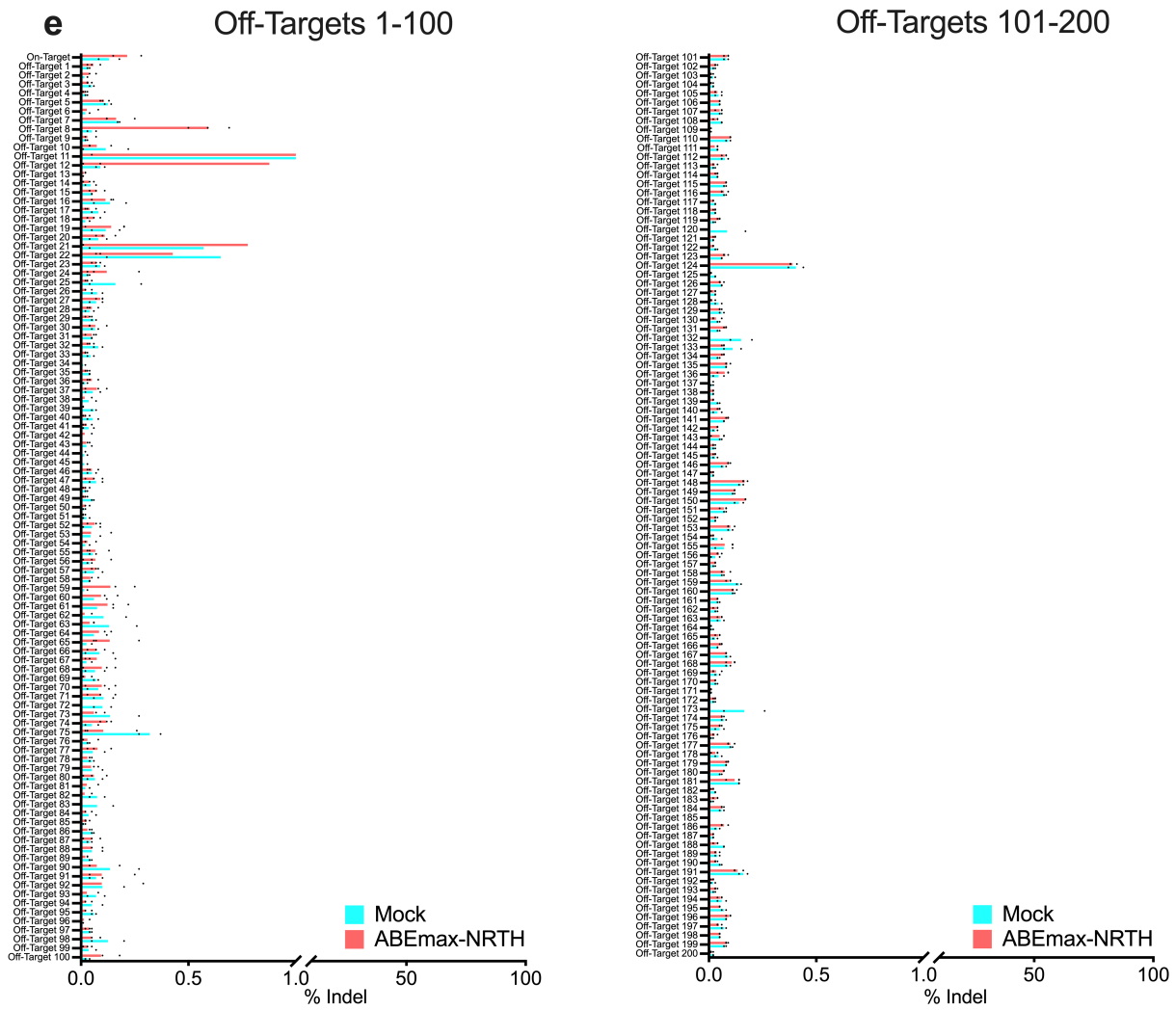

Figure S2. Base Editing of CD3δ SCID HSPCs Reveals Minimal Local Bystander and Genome-Wide Off-Target Editing and Indel Formation, Related to Fig. 2.

a) Representative flow cytometry plots to measure CD3/TCRab surface expression in *CD3D*(C202T) Jurkat T cells transduced with either LV expressing WT *CD3D* cDNA or *CD3D* cDNA containing the A0 bystander mutation. Top right: gating strategy to distinguish single cells. Bottom right: live cells. Bottom left: gating strategy to identify cells expressing CD3/TCRab. b) Venn diagram of candidate off-target sites predicted by CIRCLE-seq, GUIDE-seq, and Cas-OFFinder. Pie graph depicts the predicted genomic locations of the 57 candidate off-target sites nominated by two or more prediction tools. **c-d)** Bar graphs demonstrate the percentage of sequencing reads containing A•T-to-G•C point mutations consistent with adenine base editing and within protospacer positions 4-10 in gDNA from CD3δ SCID HSPCs treated with ABEmax-NRTH and sgRNA (peach) or untreated controls (teal). (n=3) **e)** Bar graphs demonstrate percent of sequencing reads containing indels across 200 genome-wide off-target sites. Sites were sequenced with HTS in gDNA from CD3δ SCID HSPCs treated with ABEmax-NRTH mRNA (peach) or untreated controls (teal). (n=3)

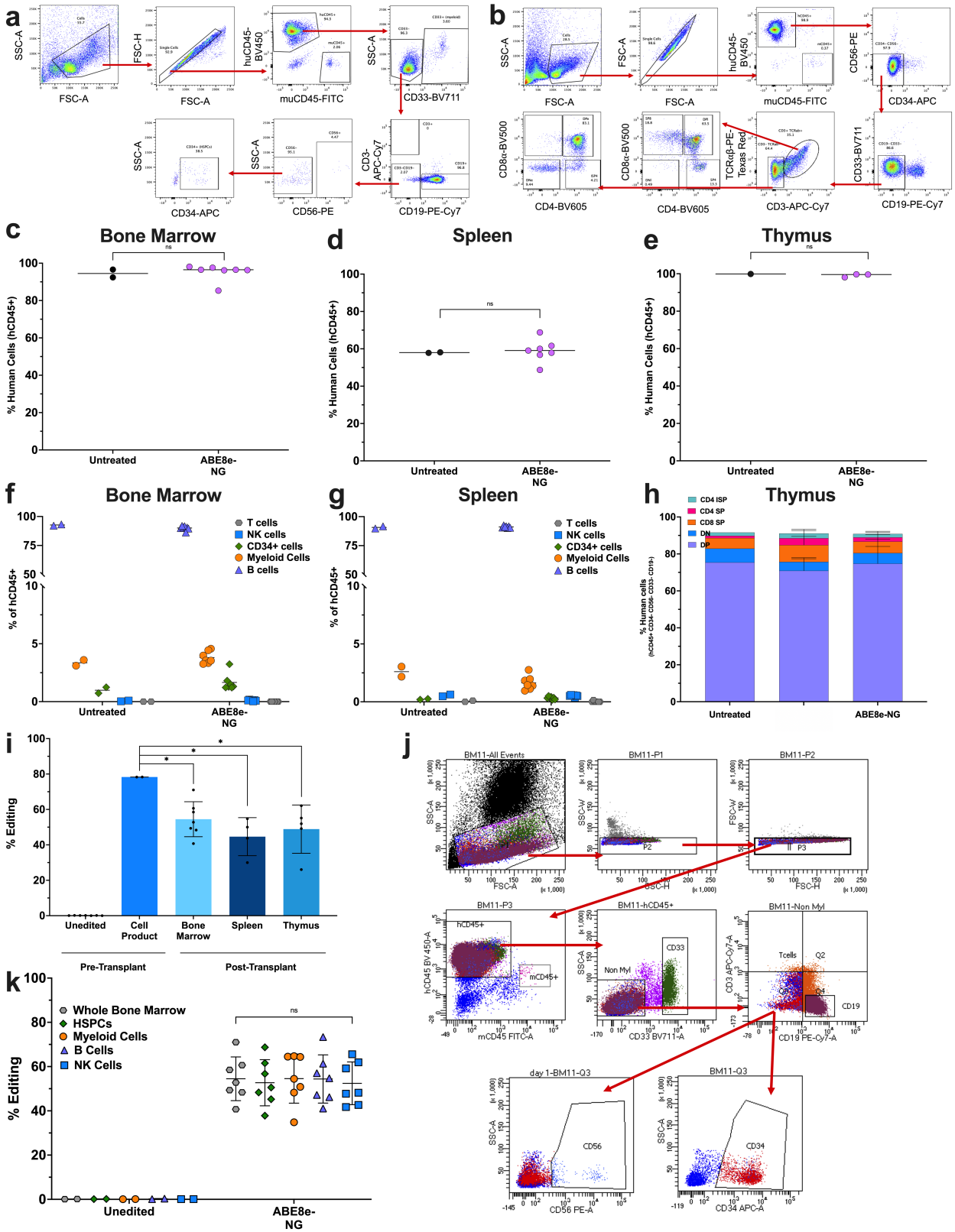
a
SSC-A
FSC-A
FSC-H
FSC-A
huCD45-BV450
muCD45-FITC
SSC-A
CD33-BV711
SSC-A
CD34-APC
SSC-A
CD56-PE
CD3-APC-Cy7
CD19-PE-Cy7
b
SSC-A
FSC-A
FSC-A
huCD45-BV450
muCD45-FITC
CD56-PE
CD34-APC
CD8α-BV500
CD4-BV605
CD8α-BV500
CD4-BV605
TCRαβ-PE-Texas Red
CD3-APC-Cy7
CD33-BV711
CD19-PE-Cy7
c
Bone Marrow
% Human Cells (hCD45+)
ns
Untreated
ABE8e-NG
d
Spleen
% Human Cells (hCD45+)
ns
Untreated
ABE8e-NG
e
Thymus
% Human Cells (hCD45+)
ns
Untreated
ABE8e-NG
f
Bone Marrow
% of hCD45+
T cells
NK cells
CD34+ cells
Myeloid Cells
B cells
Untreated
ABE8e-NG
g
Spleen
% of hCD45+
T cells
NK cells
CD34+ cells
Myeloid Cells
B cells
Untreated
ABE8e-NG
h
Thymus
CD4 ISP
CD4 SP
CD8 SP
DN
DP
% Human cells (hCD45+ CD34- CD56- CD33- CD19-)
Untreated
ABE8e-NG
i
% Editing
Unedited
Cell Product
Bone Marrow
Spleen
Thymus
Pre-Transplant
Post-Transplant
j
BM11-All Events
BM11-P1
BM11-P2
BM11-P3
BM11-hCD45+
BM11-Non Myl
hCD45+
mCD45+
Non Myl
CD33
Tcells
CD19
day 1-BM11-Q3
BM11-Q3
CD56
CD34
k
% Editing
Whole Bone Marrow
HSPCs
Myeloid Cells
B Cells
NK Cells
ns
Unedited
ABE8e-NG

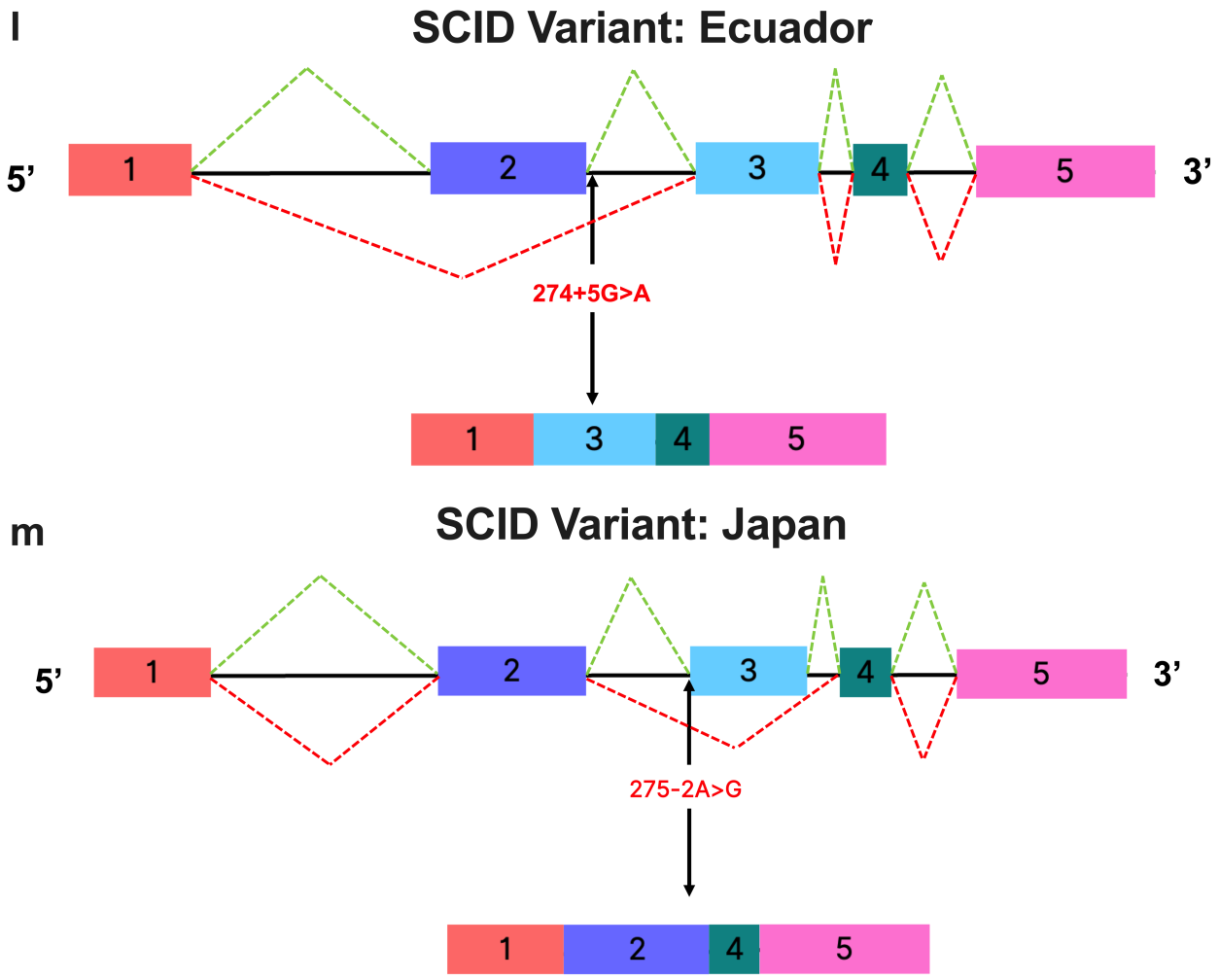

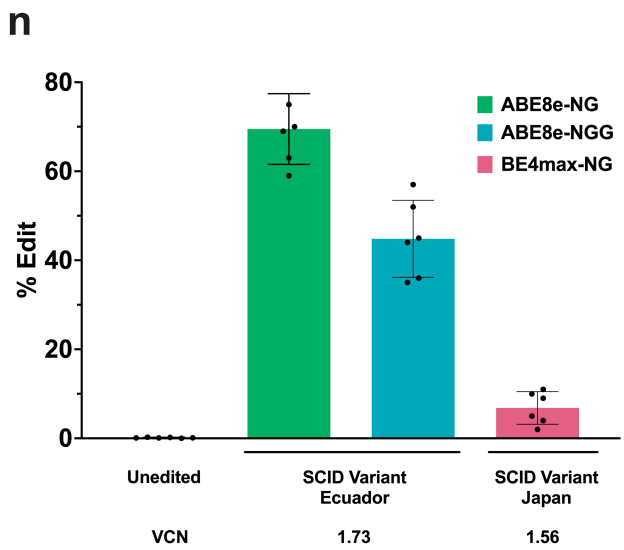

Figure S3. Base Editing is Durable in a Humanized Mouse Model and Can Rescue Additional CD3δ SCID-Causing Mutations in Human HSPCs, Related to Fig. 3.

a) Gating strategy to quantify relative abundances of hematopoietic lineages in recipient mouse bone marrow. **b)** Gating strategy to determine relative abundances of thymocytes across T cell development in recipient mouse thymi. Sixteen weeks after infusion, engraftment was measured by percentage of human CD45+ cells in recipient mouse **c)** bone marrow, **d)** spleen, and **e)** thymus for mice receiving untreated cells or ABE8e-NG treated cells. Abundance of human CD19+ B cells, CD33+ myeloid, CD34+ HSPCs, CD56+ NK cells, and CD3+ T cells were measured as percentages of the hCD45+ population in transplant recipient **f)** bone marrow and **g)** spleen. **h)** Human CD3-TCRαβ-CD4+ immature SP (CD4 ISP), CD3+TCRαβ+CD4+ (CD4 SP), CD3+TCRαβ+CD8+ single-positive (CD8 SP), CD4-CD8- double-negative (DN), and CD4+CD8+ double-positive (DP) cells as percentages of the hCD45+ population in recipient mouse thymus. **i)** *on-target* editing efficiency and VCN determined by HTS and ddPCR, respectively, in cells cultured for 14 days after electroporation (pre-transplant) or in whole tissues 16 weeks after transplant. **j)** Gating strategy for FACS isolation of CD34+ HSPCs, CD33+ Myeloid, CD19+ B cells, and CD56+ NK cells from mouse bone marrow. **k)** Editing efficiency in human-derived hematopoietic lineages from mouse bone marrow. Populations were FACS sorted using hCD34+, hCD33+, hCD19+, and hCD56+ antibodies for HSPC, myeloid, B cell, and NK cell collection, respectively. n=2 mice that received untreated cells and n=7 mice that received ABE8e-NG edited cells. Data shown as mean ± SD; **k)** one-way ANOVA, non-parametric t-test elsewhere; ns, not significant. **l)** Schematic of the splicing mutation (identified in Ecuador) known to cause CD3δ SCID. A homozygous mutation in the splice donor site of intron 2 leads to abnormal splicing and exon 2 skipping (*CD3D* c.274+5G>A).[44] **m)** Schematic of the splicing mutation, *CD3D* c.275-2A>G, (identified in Japan) known to cause CD3δ SCID.[64] A homozygous mutation in the splice acceptor site of intron 2 leads to abnormal splicing and exon 3 skipping. **n)** Healthy donor (HD) CD34+ HSPCs were pre-stimulated for 24 hours and transduced with a lentiviral vector [containing either the *CD3D* c.274+5G>A mutation (MNDU3-CD3D-274+5G>A) or *CD3D* c.275-2A>G mutation (MNDU3-CD3D-275-2A>G) in intron 2). Intron 2 was retained in the LV by positioning the internal expression cassette in reverse orientation. 24 hours after transduction, HSPCs were electroporated with ABE8e-NG, ABE8e-NGG, or BE4max-NG mRNA and sgRNA. Data shown as mean ± SD.

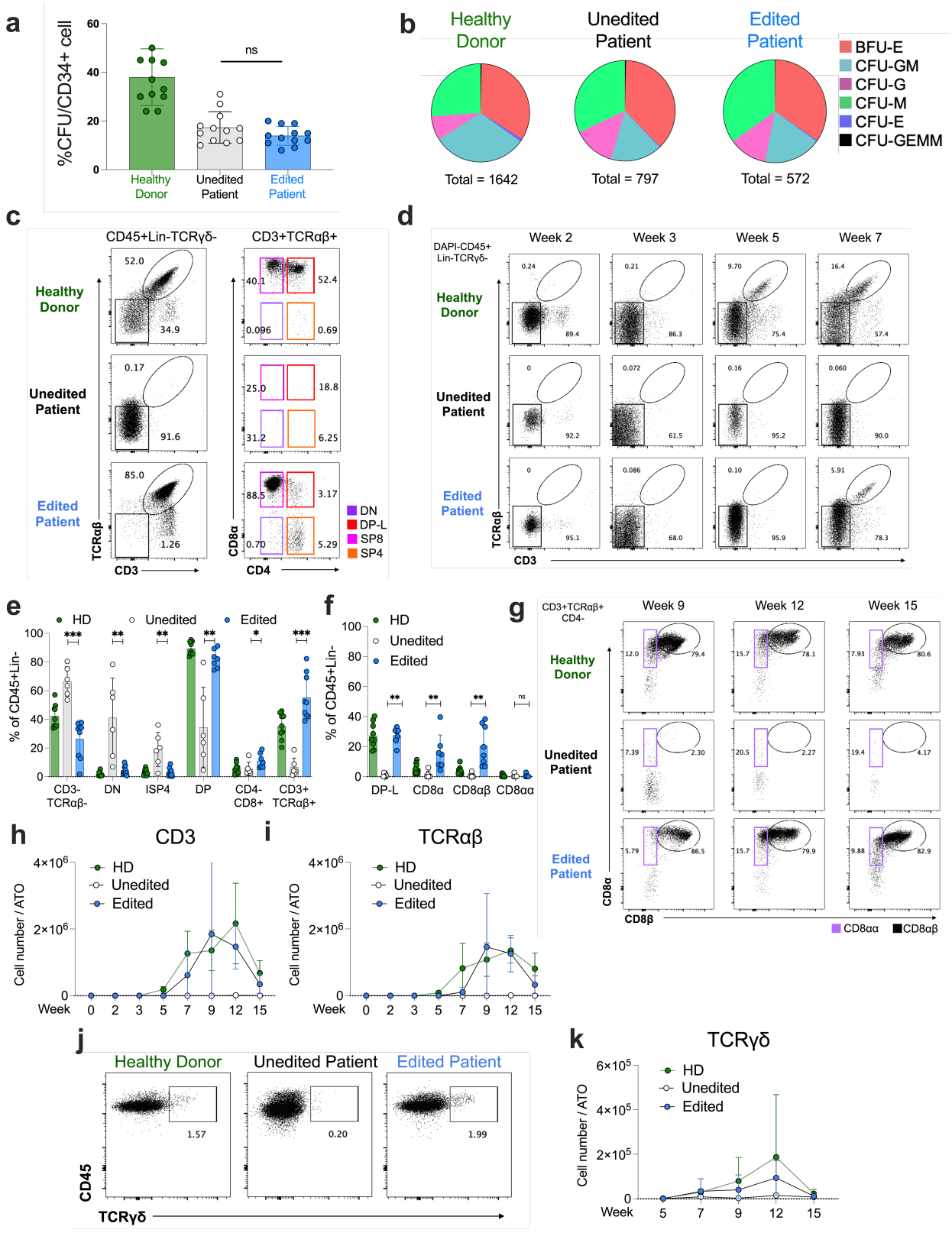

Figure S4. Base Editing Retains Clonogenic Potential and Rescues T cell Differentiation and Maturation, Related to Fig. 4.

a-b) Clonogenic potential. 24 hours following electroporation of CD3δ SCID CD34+ HSPCs, a CFU assay was performed to assess **a)** hematopoietic potential and **b)** hematopoietic lineage distribution of CD34+ HSPC HD, unedited, and edited patient T cells prior to ATO formation (n=12). Statistics were calculated using a non-parametric t-test; ns, not significant. **c-k)** Rescue of T cell differentiation. **c and d)** FACS analysis of HD (green), unedited patient (black), and edited patient (blue) ATOs, n=6-9, from four independent experiments for all data. **c)** CD3 and TCRαβ co-expression (left), and developing T cell subsets (DN, DP-L, SP8, and SP4) (right) in ATOs at week 15. **d)** Early CD3 and TCRαβ co-expression at weeks 2, 3, 5, and 7. Frequency of **e)** CD3-TCRαβ-, DN, ISP4, DP, CD4-CD8+, and CD3+TCRαβ+ cells from CD45+Lin- cells, and **f)** DP-L, CD8α, CD8αβ (SP8 T cells), and CD8αα cells from CD45+Lin- cells at week 12. **g)** Representative flow cytometry profiles of CD8αα and CD8αβ cells in cells gated on CD3+TCRαβ+CD4- in HD, unedited patient, and edited patient ATOs at weeks 9, 12, and 15. Cell counts of **h)** CD3+ and **i)** TCRαβ+ cells per ATO over time. **j)** Representative flow cytometry profiles of TCRγδ expression in cells gated on CD45+Lin- at week 12. **k)** Cell counts of γδ T cells per ATO over time. Statistical significance was calculated using unpaired nonparametric T tests, $^{**}p < 0.01$; and $^{***}p < 0.001$.

a

Cell numbers of developing T cell and immune cell subsets in unedited and edited CD3δ SCID ATOs, identified by CITE-seq.												
	CD34+	DN	ISP4	DP-E	DP-L	SP8RO	SP8RA	NK	gd	pDC	B	Total
Unedited Exp#1	114	820	5375	105	4	0	0	350	83	83	98	7000
Unedited Exp#2	52	309	3796	69	4	0	0	229	21	21	48	4561
Edited Exp#1	19	20	659	2393	1756	203	52	96	324	324	4	5530
Edited Exp#2	23	95	800	1753	1643	75	48	46	144	1	9	4637

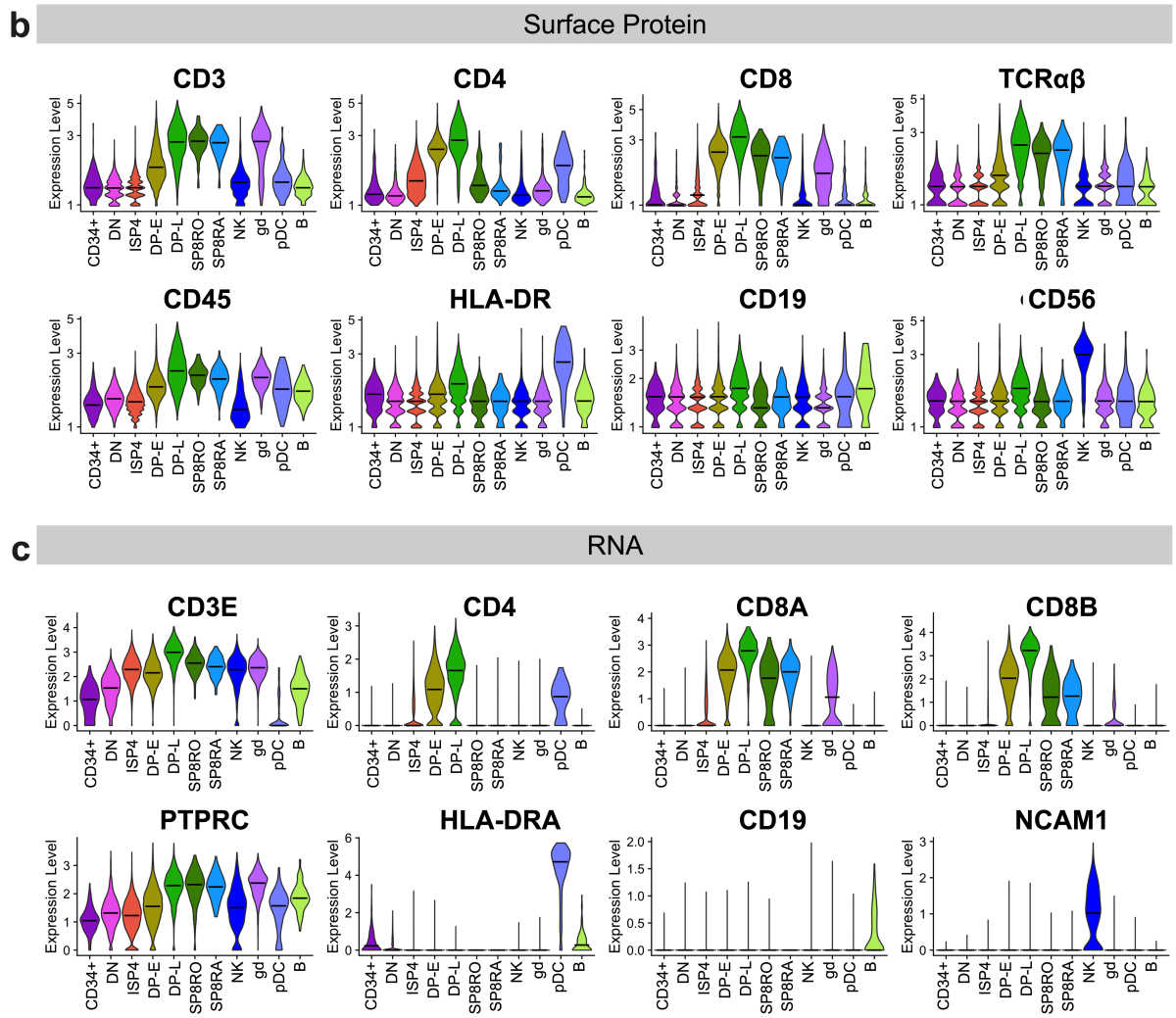

Figure S5. Identification of Developing T cell and Immune Cell Subsets in Unedited and Edited CD3δ SCID ATOs by CITE-seq, Related to Fig. 5.

a) Number of bioinformatically cleaned cells in indicated cell subsets in unedited and edited patient ATOs harvested at week 8 from two individual experiments. **b)** Surface protein and **c)** RNA gene expression of selected markers across cell subsets.

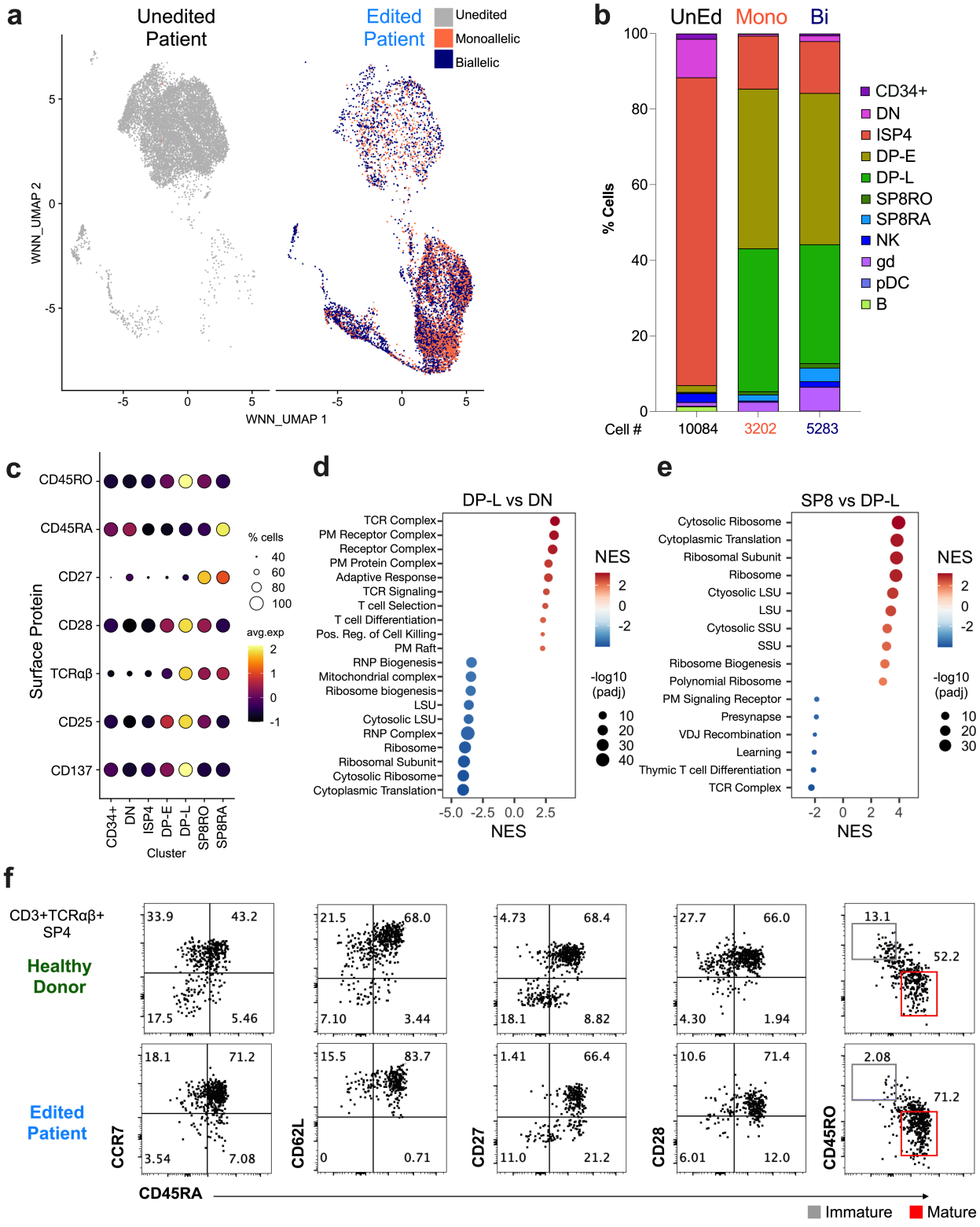
a
Unedited Patient
Edited Patient
Unedited
Monoallelic
Biallelic
WNN_UMAP 2
WNN_UMAP 1
b
UnEd
Mono
Bi
% Cells
Cell #
10084
3202
5283
CD34+
DN
ISP4
DP-E
DP-L
SP8RO
SP8RA
NK
gd
pDC
B
c
Surface Protein
CD45RO
CD45RA
CD27
CD28
TCRαβ
CD25
CD137
% cells
avg.exp
Cluster
d
DP-L vs DN
TCR Complex
PM Receptor Complex
Receptor Complex
PM Protein Complex
Adaptive Response
TCR Signaling
T cell Selection
T cell Differentiation
Pos. Reg. of Cell Killing
PM Raft
RNP Biogenesis
Mitochondrial complex
Ribosome biogenesis
LSU
Cytosolic LSU
RNP Complex
Ribosome
Ribosomal Subunit
Cytosolic Ribosome
Cytoplasmic Translation
NES
-log10 (padj)
e
SP8 vs DP-L
Cytosolic Ribosome
Cytoplasmic Translation
Ribosomal Subunit
Ribosome
Ctyosolic LSU
LSU
Cytosolic SSU
SSU
Ribosome Biogenesis
Polynomial Ribosome
PM Signaling Receptor
Presynapse
VDJ Recombination
Learning
Thymic T cell Differentiation
TCR Complex
NES
-log10 (padj)
f
CD3+TCRαβ+ SP4
Healthy Donor
Edited Patient
CCR7
CD45RA
CD62L
CD27
CD28
CD45RO
Immature
Mature

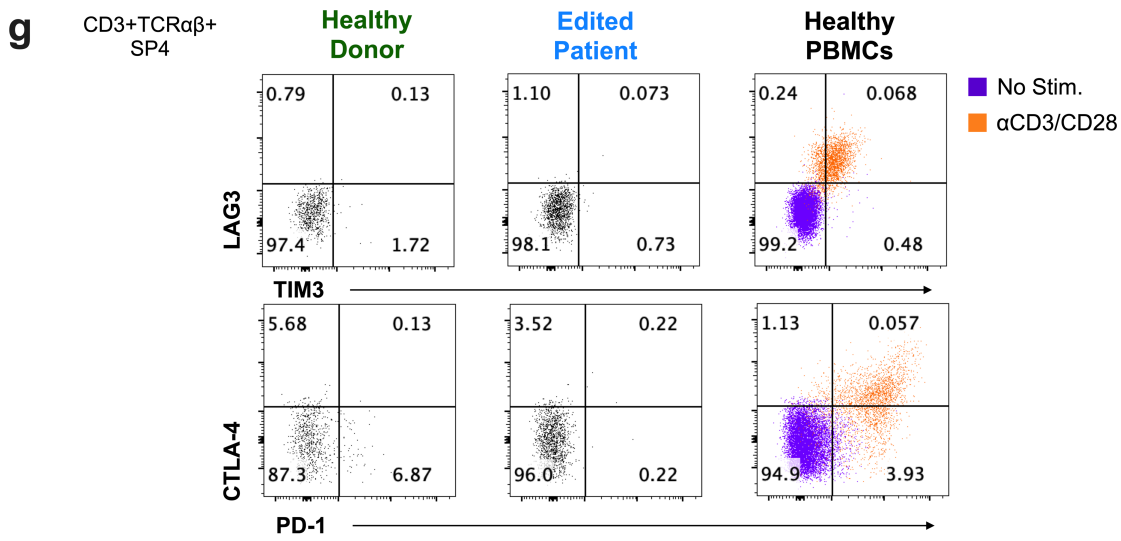

Figure S6. Monoallelic and Biallelic *CD3D* Correction Rescues SP8 and SP4 T cell Development, Related to Fig. 6.

a-b) Monoallelic and biallelic CD3*D* correction. **a)** WNN_UMAP visualization of unedited (grey), monoallelic (orange), or biallelic (blue) correction of patient ATOs. **b)** Bar graphs show relative T cell precursor abundances of binned by the presence of unedited, monoallelic, or biallelic correction in single cells. Monoallelic vs. biallelic classification was determined by the presence of RNA strands with or without the *CD3D* c.202C>T edit. UnEd, unedited; Mono, monoallelic; Bi, biallelic. **c-g)** Edited CD3δ SCID ATO-derived SP8 T and SP4 T cells express features of maturation without evidence of exhaustion**. c)** Expression of indicated surface proteins (y-axis) across clusters in edited patient ATOs. **d-e)** Gene Set Enrichment Analysis (GSEA) of differentially expressed genes from GOBP (Gene Ontology Biological Process) and GOCC (Gene Ontology Cellular Compartment) between **d)** DP-L and DN, or **e)** SP8 T and DP-L cells. Dot size represents adjusted P-value (Padj; two-sided permutation test). NES, normalized enrichment score; PM, plasma membrane; RNP, ribonucleoprotein; LSU, large ribosomal subunit; SSU, small ribosomal subunit. **f)** Representative flow cytometry profiles depicting maturation markers (CCR7, CD62L, CD27, CD28, CD45RO, and CD45RA) in cells gated on SP4 T cells - CD3+TCRαβ+CD4+CD8-, in week 12 ATOs (n=9, from four independent experiments). **g)** Representative flow cytometry profiles of exhaustion markers in SP4 T cells derived from week 15 HD (green) and edited patient (blue) ATOs, and Healthy PBMCs (right) stimulated with (orange) and without (purple) anti-CD3/28 beads + IL2 for 24 hours, n=9 for ATO groups and n=3 for PBMC controls.

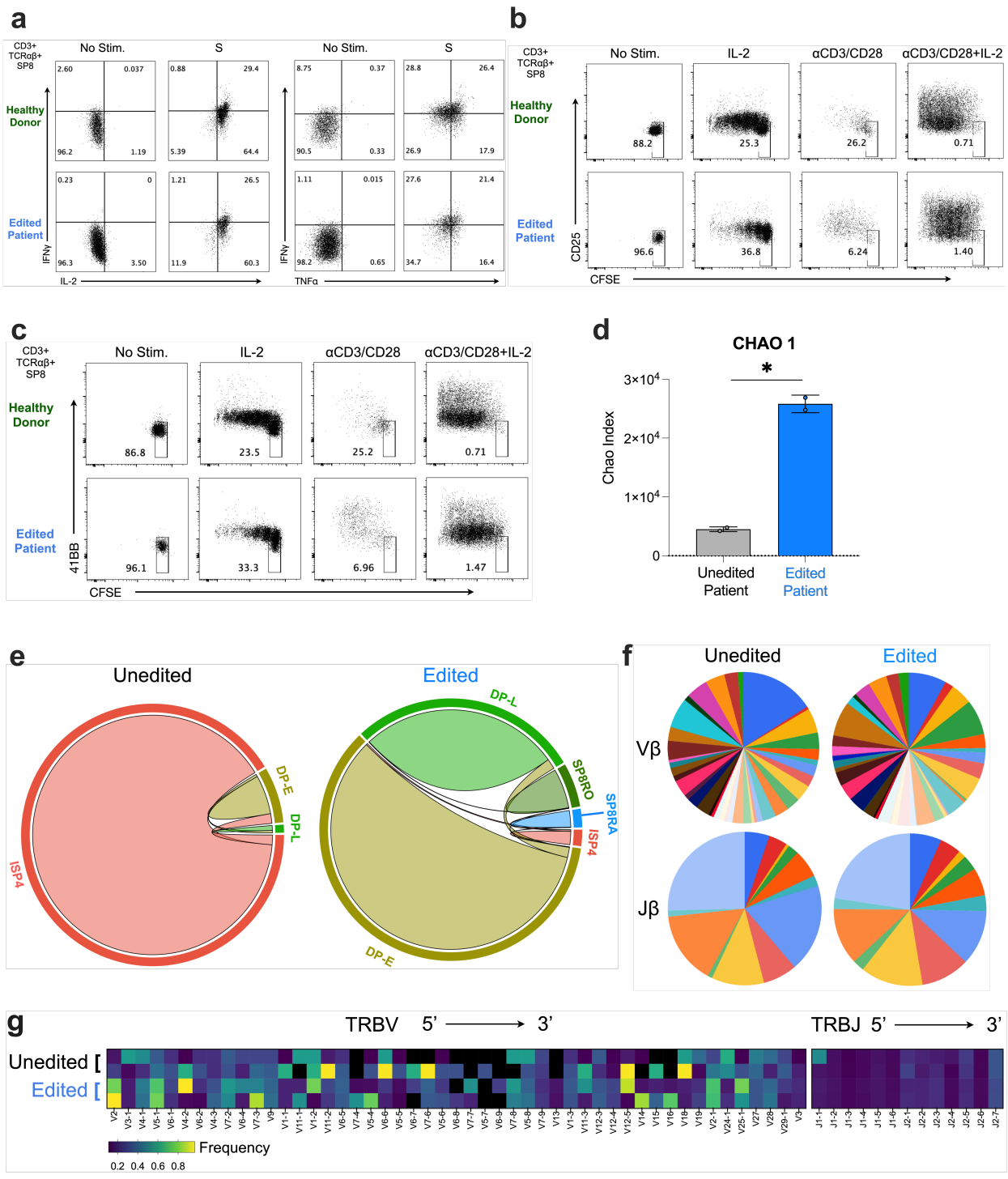

Figure S7. Base editing of CD3δ SCID HSPCs recapitulates functional T cells with TCR diversity, Related to Fig. 7.

a-c) Representative flow cytometry profiles of HD (green) and edited patient (blue) ATOs. **a)** IFNγ, IL-2, and TNFα production in SP8 T cells (CD3+TCRαβ+CD8α+CD4-CD45RA+) stimulated with or without anti-CD3/CD28 beads and IL2 for 24 hours, n=6. **b)** CD25 and **c)** 4-

1BB expression vs proliferation (CFSE dilution) of MACs isolated ATO-derived SP8 cells after culture without stim, with IL2 alone, anti-CD3/CD28 bead alone, and anti-CD3/CD28 bead + IL-2 for 5 days. Data is representative of three independent experiments. **d-h)** TCR diversity by CITE-seq of unedited (black) and edited (blue) patient ATOs harvested at week 8, n=2 per arm, two independent experiments. **d)** TCR diversity measured by CHAO-1 index. Statistical significance was calculated by Hutchinson t-test (*p<5e10-8). **e)** Chord diagrams depicting interconnection of TCR clonotypes in developing cell subsets in unedited (left) and edited (right) patient ATOs. Area of each segment correlates to the relative abundance of TCR clonotypes in indicated cells subsets. Curved lines indicate TCR clonotypes shared between cell subsets. **f)** Frequency of individual TRBV (top) and TRBJ (bottom) usage. **g)** Heatmap visualization of individual TRBV and TRBJ segments displayed in genomic order from 5' distal -> 3' proximal ends.